

Biometric Identification by Detecting Hand Veins in Infrared Images

J. C. Martínez Perales

Instituto Politécnico Nacional
Escuela Superior de Cómputo
Av. Juan de Dios Batíz, esq. Miguel Othón de Mendizábal
Ciudad de México 07320, México

R. Flores-Carapia

Instituto Politécnico Nacional
Centro de Innovación y Desarrollo Tecnológico en Cómputo
Av. Juan de Dios Batíz, esq. Miguel Othón de Mendizábal
Ciudad de México 07700, México

B. Luna-Benoso

Instituto Politécnico Nacional
Centro de Innovación y Desarrollo Tecnológico en Cómputo
Av. Juan de Dios Batíz, esq. Miguel Othón de Mendizábal
Ciudad de México 07700, México

Copyright © 2015 J. C. Martínez Perales et al. This article is distributed under the Creative Commons Attribution License, which permits unrestricted use, distribution, and reproduction in any medium, provided the original work is properly cited.

Abstract

This paper presents a methodology to implement a computational system that can identify people by the geometry of the veins of the dorsal hand from infrared images. The methodology is as follows: First, a prototype is built by a web camera with infrared LEDs that allow capture infrared images of dorsal hand. Once the images are captured, the image analysis algorithms are applied by digital image processing

in order to segment regions of interest. Once segmented images are obtained characteristics and the pattern representing each input image is formed. Since the input pattern for each image is obtained respectively, associative memory model based on cellular automata model responsible for pattern classification is constructed.

Keywords: Digital image processing, spatial domain methods, image segmentation, geometry veins dorsal hand, biometrics

1. Introduction

The word derives from the Greek biometrics bio (life) and metry (measure), inferring the meaning and measurement of life [1]. The term biometrics is adopted to encompass technologies for the identification of persons means the recognition of physical, chemical characteristics of a person's behavior or distinctive [2, 3] features. With the growth of technology applications to areas such as computer security, access control, electronic commerce and bank transfers among others, the need to create methodologies and systems capable of identifying people, thus the importance of biometrics has taken a significant direction in the activities of society [3].

Throughout history, we have developed different techniques and procedures for identifying people. Among them are identifying individual through fingerprint [4, 5, 6], using iris recognition [7, 8, 9], facial recognition [10, 11, 12], through geometry hand [13, 14, 15], by the retina [16, 17, 18] or by voice [19, 20, 21], among others. Another approach is the identification by detection of infrared images veins in either the thumb, palm or of the hand dorsal [22, 23, 24]. This technique is based on the fact that the vein pattern is unique to each person and not generally has significant changes during the stage of life (except in the case where it is in the process of growth) [25]. To capture the vascular network of the back it is required that the area is bombarded with infrared light (wavelength from 740-to 60 nm) wavelength passing through the human skin and is absorbed by the hemoglobin in the veins, Thus, when the infrared image is captured, the pattern of blood vessels containing hemoglobin is visible and appear as dark lines [26, 27, 28].

2. Basic Concepts

2.1 Digital Imaging

A digital image is a two-dimensional function $f(x, y)$ of light intensity at a point in space, where (x, y) coordinates of that point are considering the origin in the upper left of the image. Since a digital image is a function $f(x, y)$ discretized in both spatial coordinates and in brightness, often usually it represented as a two dimensional matrix $F_{ij} = (f_{ij})_{H \times W}$, where H and W represent the size of picture (H and W referring to height and width of the image respectively) with $f_{ij} = f(x_i, x_j)$. Each element of the array is called picture element or pixel. The spatial domain refers to own image plane, and the techniques in this category are based on direct manipulation of pixels of the image [29] (Figure 1).

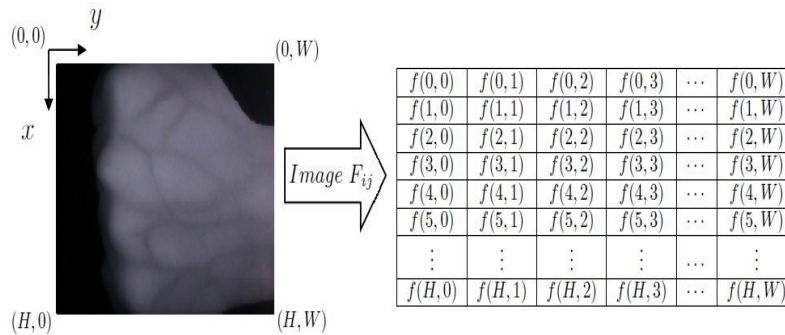


Fig. 1: Digital image.

2.2 Associative Memories

Associative memories are mathematical models whose main objective is to recover complete patterns from input patterns. The operation of the associative memories is divided into two phases: learning stage where the associative memory is generated; and recovery phase, stage where the associative memory is operated.

During the learning phase, the associative memory is constructed from a set of ordered pairs of patterns known in advance, called fundamental set. Each pattern that defines the fundamental set is called central pattern. Fundamental set is represented as follows [30, 31]:

$$FS = \{(\mathbf{x}^\mu, \mathbf{y}^\mu) | \mu = 1, 2, \dots, p\} \quad (1)$$

where $(\mathbf{x}^\mu, \mathbf{y}^\mu) \in A^n \times A^m$ for $\mu = 1, 2, \dots, p$, with $A = \{0, 1\}$.

During the recovery stage, associative memory operating with an input pattern for the corresponding output pattern.

2.3 Cellular Automata

Let I be a set of indices. Let $A = \{[a_i, b_i]\}_{i \in I}$ countable family of closed intervals in \mathbb{R} such that the following conditions:

1. $\bigcup_{X \in A} X = [a, b]$ for some $a, b \in \mathbb{R}$ o $\bigcup_{X \in A} X = \mathbb{R}$.
2. if $[a_i, b_i] \in A$, then $b_i - a_i > 0$.
3. if $[a_i, b_i]$ and $[c_j, d_j]$ are in A with $b_i \leq c_j$, then $[a_i, b_i] \cap [c_j, d_j] = \emptyset$ or $[a_i, b_i] \cap [c_j, d_j] = b_i = c_j$.

Definition. Let $[a, b]$ an interval of \mathbb{R} with $a \neq b$ and A a family of closed intervals that satisfy 1, 2 and 3. A 1-dimensional lattice is the set $\mathcal{L} = \{x_i \times [a, b] \mid x_i \in A\}$. If A_1, A_2, \dots, A_n are families of intervals that meets 1, 2 and 3, then a lattice of dimension $n > 1$ is the set $\mathcal{L} = \{x_1 \times x_2 \times \dots \times x_n \mid x_i \in A_i\}$.

Definition. Let $r \in \mathbb{R}$. An 1-dimensional lattice is regular if $[a_i, b_i] = r$ for each $[a_i, b_i] \in A$. An n -dimensional lattice is *regular* if $[a_{i_k}, b_{i_k}] = r$ for each $[a_{i_k}, b_{i_k}] \in A_i$ for $i = 1, 2, \dots, n$.

Definition. Let \mathcal{L} be a lattice. A cell or site is an element of \mathcal{L} , that is, a cell is an element of the form $[a_{1_k}, b_{1_k}] \times \dots \times [a_{n_k}, b_{n_k}]$ with $[a_{i_k}, b_{i_k}] \in A_i$ for $i = 1, 2, \dots, n$.

Definition. Let \mathcal{L} be a lattice, and r is a cell of \mathcal{L} . A neighborhood of size $n \in \mathbb{N}$ for r , is the set $v(r) = \{\{k_1, k_2, \dots, k_n\} \mid k_j \text{ is a cell of } \mathcal{L} \text{ for each } j\}$.

Definition. Let $n \in \mathbb{N}$. A cellular automaton is a tuple $(\mathcal{L}, \mathcal{S}, \mathcal{N}, f)$ such that:

1. \mathcal{L} is a regular lattice.
2. \mathcal{S} is a finite set of states.
3. \mathcal{N} is a set of neighborhoods nest as follows:

$$\mathcal{N} = \{v(r) \mid r \text{ is a cell and } v(r) \text{ is a neighborhood } r \text{ of size } n\}$$

4. $f : \mathcal{N} \rightarrow \mathcal{S}$ is a function called the transition function.

Definition. A configuration of the cellular automaton $(\mathcal{L}, \mathcal{S}, \mathcal{N}, f)$ is a function $C_t : \mathcal{L} \rightarrow \mathcal{S}$ which associates to each cell of the lattice \mathcal{L} at time t , a state of \mathcal{S} .

If $(\mathcal{L}, \mathcal{S}, \mathcal{N}, f)$ is a cellular automaton and $r \in \mathcal{L}$, then the configuration C_t is related with f through:

$$C_t = f(\{C_t(i) | i \in \mathcal{N}(r)\})$$

Definition. Let $\mathcal{Q} = (\mathcal{L}, \mathcal{S}, \mathcal{N}, f)$ and $\mathcal{W} = (\mathcal{L}, \mathcal{S}, \mathcal{N}', g)$ two cellular automata. Cellular automaton composition of the CA \mathcal{Q} and \mathcal{W} in the time $t = t_k$ is defined as $\mathcal{W} * \mathcal{Q}$ by the cellular automaton $\mathcal{W} * \mathcal{Q} = (\mathcal{L}, \mathcal{S}, \mathcal{N}, h)$ where h , f and g are related as follows:

$$C_{t_k+1}(r) = f(\{C_{t_k}(i) : i \in \mathcal{N}(r)\})$$

$$C_{t_k+2}(r) = g(\{C_{t_k+1}(i) : i \in \mathcal{N}'(r)\})$$

$$C_{t_k+2}(r) = h(\{C_{t_k}(i) : i \in \mathcal{N}(r)\})$$

Definition. Let $\mathcal{R} = (\mathcal{L}, \mathcal{S}, \mathcal{N}, f)$ a cellular automaton with $\mathcal{L} = \mathbb{Z}^2$. If $A \subseteq \mathbb{Z}^2$ and $x \in \mathcal{S}$, then $[A]_x$ denote the number of cells in A with state x .

2.4 Associative Memories based on Cellular Automata

In this work was used the associative memory model based on cellular automata by the authors in [32]. Then previous definitions and the proposed model are presented.

Definition. Let $A, B \subseteq \mathbb{Z}^2$. The cell dilation is the cellular automata $\mathcal{D} = (\mathcal{L}, \mathcal{S}, \mathcal{N}, f)$ whit initial configuration A , defined as follows:

- $\mathcal{L} = \mathbb{Z}^2$.
- $\mathcal{S} = \{0, 1\}$.
- $\mathcal{N} = \{v_x | x \in \mathcal{L}\}$ with $v_x = (B^-)_x = \{-b + x | b \in B\}$.
- The transition function $f : \mathcal{N} \rightarrow \mathcal{S}$ is given as follows:

$$f(v_x) = \begin{cases} 1 & \text{if } [v_x]_1 > 0 \\ 0 & \text{if } [v_x]_1 = 0 \end{cases}$$

Definition. Let $A, B \subseteq \mathbb{Z}^2$. . The cell erosion is the cellular automata $\mathcal{D} = (\mathcal{L}, S, \mathcal{N}, f)$ with initial configuration A , defined as follows:

- $\mathcal{L} = \mathbb{Z}^2$.
- $S = \{0, 1\}$.
- $\mathcal{N} = \{v_x | x \in \mathcal{L}\}$ with $v_x = (B)_x = \{b + x | b \in B\}$.
- The transition function $f : \mathcal{N} \rightarrow S$ is:

$$f(v_x) = \begin{cases} 1 & \text{if } [v_x]_1 = |B| \\ 0 & \text{if } [v_x]_1 < |B| \end{cases}$$

In what follows, consider the set $A = \{0, 1\}$ and the fundamental set $FS = \{(\mathbf{x}^\mu, \mathbf{y}^\mu) | \mu = 1, 2, \dots, p\}$ with $\mathbf{x}^\mu \in A^n$ and $\mathbf{y}^\mu \in A^m$.

The lattice \mathcal{L} for the CA shall consist of the matrix of size $2m \times 2n$ with the first index in $(0, 0)$.

The set $S = \{0, 1\}$ is the finite set of states.

Let $I = \{i \in \mathbb{Z} | i = 2k \text{ for } k = 0, 1, 2, \dots, n - 1\} = \{0, 2, 4, \dots, 2(n) - 2\}$ and $J = \{j \in \mathbb{Z} | j = 2k + 1 \text{ for } k = 0, 1, 2, \dots, m - 1\} = \{1, 3, 5, \dots, 2m - 1\}$. Consider the partition of \mathcal{L} formed by the family of subsets $IJ = \{v_{(i,j)} | (i, j) \in I \times J\}$ with $v_{(i,j)} = \{(i, j), (i, j - 1), (i + 1, j), (i + 1, j - 1)\}$. Since IJ is a partition of \mathcal{L} , given $\mathbf{l} \in \mathcal{L}$, exists a unique $(i, j) \in I \times J$ such that $\mathbf{l} \in v_{(i,j)}$. We denote by $v^{\mathbf{l}}$ this single element, i.e. $v^{\mathbf{l}} = v_{(i,j)}$. For example, if $\mathbf{l} = (3, 0)$ then $\mathbf{l} \in v^{(3,0)} = v_{(2,1)} = \{(2, 1), (2, 0), (3, 1), (3, 0)\}$.

From the above fact it defines the set of neighborhoods

$$\mathcal{N} = \{v^{\mathbf{l}} | \mathbf{l} \in \mathcal{L}\} \tag{2}$$

Definition. Consider the set A^k . We define the projection function of the i -th component ($1 \leq i \leq k$) as $Pr_i : A^k \rightarrow A$ as:

$$Pr_i(\mathbf{z}) = z_i, \text{ with } \mathbf{z} = (z_1, z_2, \dots, z_k) \tag{3}$$

Theorem. If $(y_i, x_j) \in Pr_{\mathbf{y}\mathbf{x}} = \{(y_i, x_j) | y_i = Pr_i(\mathbf{y}) \text{ and } x_j = Pr_j(\mathbf{x})\}$, then $(2j - 2 + y_i, 2i - 2 + x_j) \in v_{(2j-2, 2i-1)}$.

We define the set $\mathcal{L}_{FS} = \{(2j - 2 + y_i^\mu, 2i - 2 + x_j^\mu) | 1 \leq \mu \leq p, 1 \leq i \leq m \text{ and } 1 \leq j \leq n\} \subseteq \mathcal{L}$.

Consider the CA $\mathcal{Q} = (\mathcal{L}, \mathcal{S}, \mathcal{N}, f_{\mathcal{Q}})$ and $\mathcal{W} = (\mathcal{L}, \mathcal{S}, \mathcal{N}', f_{\mathcal{W}})$ with $\mathcal{N}' = IJ$, and $f_{\mathcal{Q}} : \mathcal{N} \rightarrow S$, $f_{\mathcal{W}} : \mathcal{N}' \rightarrow S$ defined as follows:

$$f_{\mathcal{Q}}(v^{(i,j)}) = \begin{cases} 1 & \text{if } (i, j) \in \mathcal{L}_{FS} \\ 0 & \text{if } (i, j) \notin \mathcal{L}_{FS} \end{cases}$$

$$f_{\mathcal{W}}(v_{(i,j)}) = \begin{cases} 1 & \text{in position } (i + 1, j) \text{ if } (i, j - 1) = 1 \\ 1 & \text{in position } (i, j - 1) \text{ if } (i + 1, j) = 1 \end{cases}$$

We define the Associative CA (ACA) in its learning phase as

$$\mathcal{W} * \mathcal{Q} = (\mathcal{L}, \mathcal{S}, \mathcal{N}, f_A) \quad (4)$$

The recovery phase for the ACA makes use of the composition of erosions and dilations CA. The algorithm which defines the phase of recovery is shown in algorithm 1.

Algorithm 1 ACA in recovery phase

Fundamental set $FS = \{(\mathbf{x}^\mu, \mathbf{y}^\mu) | \mu = 1, 2, \dots, p\}$; structuring element B ; integer value ne (number of erosions); integer value nd (number of dilations); pattern to recovery $\tilde{\mathbf{x}} \in A^n$ Recovery pattern $\tilde{\mathbf{y}} \in A^m$

1. Building the Learning ACA for FS .
2. Applying ne times the cell erosion \mathcal{E} with the structuring element B to the initial configuration of learning ACA. This is, applied to the configuration of the ACA, $\mathcal{E} * \mathcal{E} * \dots * \mathcal{E}$, ne times.
3. Applying nd times the cellular dilation with the structuring element \mathcal{D} to configuration obtained in point 2. This is, applied to the configuration obtained in point 2, $\mathcal{D} * \mathcal{D} * \dots * \mathcal{D}$, nd times.
4. For the input pattern $\tilde{\mathbf{x}} \in A^n$ will get the output pattern $\tilde{\mathbf{y}} \in A^m$ applying:

$i = 1 \rightarrow m \tilde{y}_i = 1 \ j = 1 \rightarrow n \neg(\tilde{x}_j = 0 \wedge (2j - 1, 2i - 2) = 1) \neg(\tilde{x}_j = 1 \wedge ((2j - 2, 2i - 2) = 1 \vee (2j - 1, 2i - 2) = 1)) \tilde{y}_i = 0 \text{ Break}$

3. Proposed Method

3.1 Prototype to capture infrared images

For the proposed methodology, first a prototype was made that is capable of storing infrared images of the hand dorsal, for it, a metal structure support was used for a lamp, a web camera with an infrared filter, 70 LEDs infrared of 5mm diameter was used model IR333, 10 resistors of 470 Ohm, a potentiometer of 10k and a bridge rectifier. An array of infrared LEDs was constructed for the illumination of the back of the hand, regulating the intensity of the LEDs by the potentiometer; bridge rectifier circuit is powered by an alternating current of 120V-60Hz. The web camera was placed at the center of the array of LEDs to capture images of the hand dorsal when it was bombed by infrared light. Figure 2 shows the circuit of the LED matrix, and the rectifying circuit for connecting alternating current. Figure 3 shows the prototype that captures infrared images of the hand dorsal.

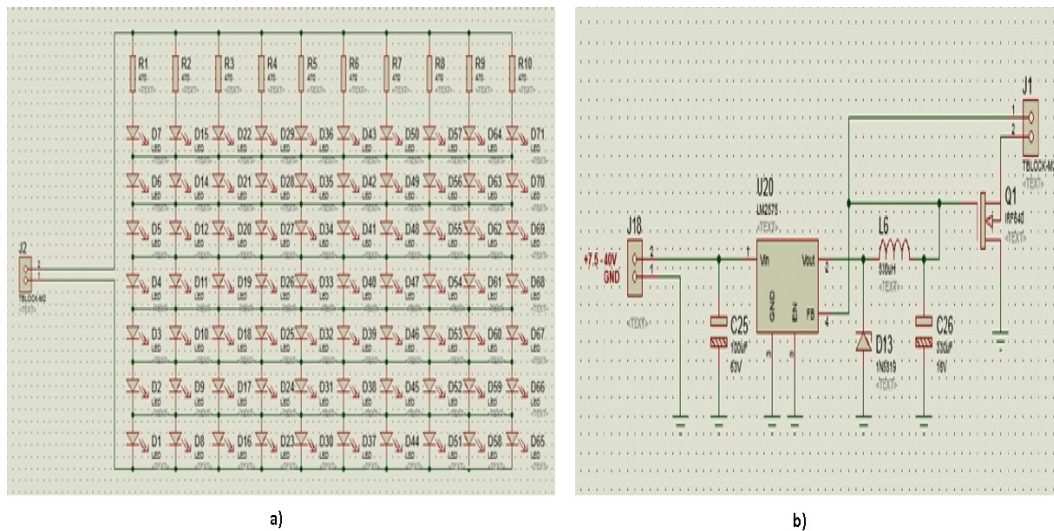


Fig. 2: In a) matrix circuit LEDs, and in b) rectifier circuit to connect the alternate current



Fig. 3: Capture infrared images of the back of the hand.

3.2 Digital Image processing

Once developed the prototype of Section 3.1, proceeded to capture images of the back of the left hand. For each of the captured images the hand was segment as follows: given the infrared light image obtained, the histogram is considered and the two absolute maxima of the histogram is calculated as shown in Figure 4 c). After obtaining the two absolute maxima, the relative minimum was calculated between the absolute maxima getting a *min* value, then the image is binarizo follows:

$$f_{ij} = \begin{cases} a & \text{si } f_{ij} > umbral \\ b & \text{si } f_{ij} \leq umbral \end{cases}$$

where $umbral = min$, $a = 0$ y $b = 255$. Figure 4 shows the segmentation of the dorsal hand using absolute highs.

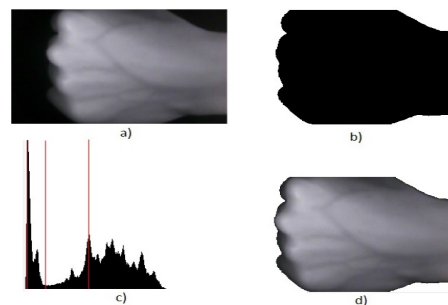


Fig. 4: Digital image processing using absolute maximums.

3.3 Feature Extraction

Once the segmentation of infrared image was obtained of the hand dorsal, we proceeded to form the pattern of features from the segmented image histogram. To do this, consider the histogram of the image 5, the value is calculated where the maximum absolute max is located and consider the values in the range $[max - 10, max + 10]$, is calculated, so that if $histo(i)$ is the corresponding value in the histogram for i with $0 \leq i \leq 255$, then the pattern corresponding to the image is given by:

$$\mathbf{x} = \begin{pmatrix} histo(max - 10) \\ histo(max - 9) \\ \dots \\ histo(max + 9) \\ histo(max + 10) \end{pmatrix}$$

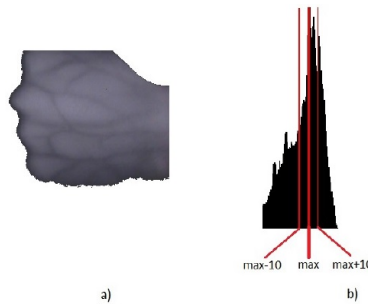


Fig. 5: Feature extraction.

3.4 Pattern recognition

After obtaining the pattern of characteristics for each of the images, associative memories based on cellular automata was implemented shown in section 2.4.

4. Experiments and results

The prototype shown in section 3.1 was built, and from this, a bank of infrared images of the left hand dorsal was created as follows: 10 people were considered, each person had 10 different images of the left hand dorsal, obtaining a

total of 100 images. This bank of images were applied the proposed methodology segmentation and feature extraction. For pattern recognition module of associative memory was used the model based on cellular automata presented in Section 2.3. The method was validated by cross validation, which is to partition the total set in k blocks of the same size, with each pass, each block plays the role of the training set and the remaining ($k - 1$ blocks) form the test set obtaining k passes in total. In each pass the model performance is recorded, and the total average of the last k passes equals the performance of the model, in this case a yield of 84.7% was obtained.

5. Conclusions

This work presented a methodology for biometric identification of people by the geometry of the veins of the dorsal hand from infrared images. First prototype was built using infrared LEDs and a modified webcam through an infrared filter to allow capturing infrared images, through this prototype infrared images of dorsal hand were captured, thus an images bank was created of the veins geometry of the dorsal hand of different people, once created the images bank, we applied the methodology able to segment each of the vascular network of the dorsal hand, features were extracted and associative memory was created based on cellular automata. The methodology was applied to each of the images of the images Bank and the model was validated by cross validation, obtaining a yield of 84.7%.

Acknowledgements. The authors would like to thank the Instituto Politécnico Nacional (Secretaría Académica, EDI, EDD, COFAA, SIP, ESCOM and CIDETEC), the CONACyT and SNI for their economical support to develop this work.

References

- [1] A. Sánchez, *Aplicaciones en la Visión Artificial y la Biometría Informática*, Universidad Rey Juan Carlos, primera edición, Librería editorial Dykinson, 2005.
- [2] Egon L. van den Broek, Beyond Biometrics, *Procedia Computer Science*, **1** (2010), no. 1, 2511-2519.
<http://dx.doi.org/10.1016/j.procs.2010.04.284>

- [3] K. Yang, E. Yingzi, Z. Zhou, Consent biometrics, *Neurocomputing*, **100** (2012), 153-162. <http://dx.doi.org/10.1016/j.neucom.2011.12.044>
- [4] M. Liu, P. Yap, Invariant representation of orientation fields for fingerprint indexing, *Pattern Recognition*, **45** (2012), no. 7, 2532-2542. <http://dx.doi.org/10.1016/j.patcog.2012.01.014>
- [5] J. Guo, Y. Liu, J. Chang, J. Lee, Fingerprint classification based on decision tree from singular points and orientation field, *Expert Systems with Applications*, **41** (2014), no. 2, 752-764. <http://dx.doi.org/10.1016/j.eswa.2013.07.099>
- [6] N. M. E. Anthonioz, C. Champod, Evidence evaluation in fingerprint comparison and automated fingerprint identification systems-Modeling between finger variability, *Forensic Science International*, **235** (2014), 86-101. <http://dx.doi.org/10.1016/j.forsciint.2013.12.003>
- [7] K. Y. Shin, G. P. Nam, D. S. Jeong, D. H. Cho, B. J. Kang, K. R. Park, Jaihie Kim, New iris recognition method for noisy iris images, *Pattern Recognition Letters*, **33** (2012), no. 8, 991-999. <http://dx.doi.org/10.1016/j.patrec.2011.08.016>
- [8] P. Li, H. M. Li, H. Ma, Iris recognition in non-ideal imaging conditions, *Pattern Recognition Letters*, **33** (2012), no. 8, 1012-1018. <http://dx.doi.org/10.1016/j.patrec.2011.06.017>
- [9] D. M. Rankin, B. W. Scotney, P. J. Morrow, B. K. Pierscionek, Iris recognition failure over time: The effects of texture, *Pattern Recognition*, **45** (2012), no. 1, 145-150. <http://dx.doi.org/10.1016/j.patcog.2011.07.019>
- [10] S. Wan, J. K. Aggarwal, Spontaneous facial expression recognition: A robust metric learning approach, *Pattern Recognition*, **47** (2014), no. 5, 1859-1868. <http://dx.doi.org/10.1016/j.patcog.2013.11.025>
- [11] E. Owusu, Y. Zhan, Q. R. Mao, A neural-AdaBoost based facial expression recognition system, *Expert Systems with Applications*, **41** (2014), no. 7, 3383-3390. <http://dx.doi.org/10.1016/j.eswa.2013.11.041>
- [12] G. K. O. Michael, T. Connie, A. B. J. Teoh, A contactless biometric system using multiple hand features, *Journal of Visual Communication and Image Representation*, **23** (2012), no. 7, 1068-1084. <http://dx.doi.org/10.1016/j.jvcir.2012.07.004>

- [13] J. Wu, Z. Qiu, D. Sun, A hierarchical identification method based on improved hand geometry and regional content feature for low-resolution hand images, *Signal Processing*, **88** (2008), no. 6, 1447-1460. <http://dx.doi.org/10.1016/j.sigpro.2007.12.007>
- [14] R. M. Luque-Baena, D. Elizondo, E. López-Rubio, E. J. Palomo, T. Watson, Assessment of geometric features for individual identification and verification in biometric hand systems, *Expert Systems with Applications*, **40** (2013), no. 9, 3580-3594. <http://dx.doi.org/10.1016/j.eswa.2012.12.065>
- [15] C. Mariño, M. G. Penedo, M. Penas, M. J. Carreira, F. Gonzalez, Personal authentication using digital retinal images, *Pattern Anal Applic.*, **9** (2006), 21-33. <http://dx.doi.org/10.1007/s10044-005-0022-6>
- [16] C. Köse, C. Ikibas, A personal identification system using retinal vasculature in retinal fundus images, *Expert Systems with Applications*, **38** (2011), no. 11, 13670-13681. <http://dx.doi.org/10.1016/j.eswa.2011.04.141>
- [17] M. Ortega, M. G. Penedo, J. Rouco, N. Barreira, M. J. Carreira, Personal verification based on extraction and characterisation of retinal feature points, *Journal of Visual Languages & Computing*, **20** (2009), no. 2, 80-90. <http://dx.doi.org/10.1016/j.jvlc.2009.01.006>
- [18] I. Bhattacharya, P. Ghosh, S. Biswas, Offline Signature Verification Using Pixel Matching Technique, *Procedia Technology*, **10** (2013), 970-977. <http://dx.doi.org/10.1016/j.protcy.2013.12.445>
- [19] B. Beranek, Voice biometrics: success stories, success factors and what's next, *Biometric Technology Today*, **2013** (2013), no. 7, 9-11. [http://dx.doi.org/10.1016/s0969-4765\(13\)70128-0](http://dx.doi.org/10.1016/s0969-4765(13)70128-0)
- [20] B. Morgen, Voice biometrics for customer authentication, *Biometric Technology Today*, **2012** (2012), no. 2, 8-11. [http://dx.doi.org/10.1016/s0969-4765\(12\)70054-1](http://dx.doi.org/10.1016/s0969-4765(12)70054-1)
- [21] M. Hashiyada, Y. Itakura, T. Nagasima, J. Sakai, M. Funatyama, High-throughput SNP analysis for human identification, DNA Polymorphism, 2007.
- [22] M. Shanin, A. Badawi, M. Kamel, Biometric Authentication Using Fast Correlation of Near Infrared Hand Vein Patterns, *International Journal of Biological and Medical Science*, **2** (2007), no. 3, 141-148.

- [23] G. Yang, X. Xi, Y. Yin, Finger Vein Recognition Based on a Personalized Best Bit Map, *Sensors*, **12** (2012), 1738-1757.
<http://dx.doi.org/10.3390/s120201738>
- [24] S. Damavandinejadmonfareda, A. K. Mobarakeh, S. A. Suandi, B. A. Rosdi, Evaluate and Determine the Most Appropriate Method to Identify Finger Vein, *Procedia Engineering*, **41** (2012), 516-521.
<http://dx.doi.org/10.1016/j.proeng.2012.07.206>
- [25] I. Sarkar, F. Alisherov, T. Kim, Debnath Bhattacharyya, Palm Vein Authentication System: A Review, *International Journal of Control and Automation*, **3** (2010), no. 1, 27-34.
- [26] B. Prasanalakshmi, A. Kannammal, B. Gomathi, K. Deepa, R. Sridevi, Biometric Cryptosystem Involving Two Traits And Palm Vein As key, *Procedia Engineering*, **30** (2012), 303-310.
<http://dx.doi.org/10.1016/j.proeng.2012.01.865>
- [27] D. Prasanna, P. Neelamegam, S. Sriram, N. Raju, Enhancement of vein patterns in hand image for biometric and biomedical application using various image enhancement techniques, *Procedia Engineering*, **38** (2012), 1174-1185. <http://dx.doi.org/10.1016/j.proeng.2012.06.149>
- [28] M. Heenaye, M. Khan, A Multimodal Hand Vein Biometric based on Score Level Fusion, International Symposium on Robotics and Intelligent Sensors 2012 (IRIS 2012), *Procedia Engineering*, **41** (2012), 897-903.
<http://dx.doi.org/10.1016/j.proeng.2012.07.260>
- [29] R. González, R. Woods, *Digital Image Processing*, 3rd ed., Prentice Hall, New Jersey, 2008.
- [30] I. López-Yáñez, I. Román-Godínez, C. Yáñez-Márquez, Classifying Patterns in Bioinformatics Databases by Using Alpha-Beta Associative Memories, *Biomedical Data and Applications*, Springer, Vol 224, 2009, 187-210.
http://dx.doi.org/10.1007/978-3-642-02193-0_8
- [31] H. Sossa, R. A. Vázquez, Behavior of morphological associative memories with true-color image patterns, *Neurocomputing*, **73** (2009), no. 1-3, 225-244. <http://dx.doi.org/10.1016/j.neucom.2009.09.004>
- [32] R. Flores-Carapia, B. Luna-Benoso, C. Yáñez Márquez, Associative Memories Based on Cellular Automata: An Application to Pattern Recognition, *Applied Mathematical Sciences*, **7** (2013), no. 18, 857-866.

Received: July 30, 2015; Published: November 5, 2015